Human Molecular Genetics, 2006, Vol. 15, No. 7 ***1195–1207***
doi:10.1093/hmg/ddl035
Advance Access published on February 23, 2006

SRPX2 mutations in disorders of language cortex and cognition

Patrice Roll[1,10], Gabrielle Rudolf[3], Sandrine Pereira[1], Barbara Royer[1], Ingrid E. Scheffer[6], Annick Massacrier[1], Maria-Paola Valenti[3], Nathalie Roeckel-Trevisiol[1], Sarah Jamali[1], Christophe Beclin[7], Caroline Seegmuller[3], Marie-Noëlle Metz-Lutz[3,8], Arnaud Lemainque[9], Marc Delepine[9], Christophe Caloustian[9], Anne de Saint Martin[4], Nadine Bruneau[2], Danièle Depétris[1], Marie-Geneviève Mattéi[1], Elisabeth Flori[5], Andrée Robaglia-Schlupp[1,10], Nicolas Lévy[1,11], Bernd A. Neubauer[12], Rivka Ravid[13], Christian Marescaux[3], Samuel F. Berkovic[6], Edouard Hirsch[3], Mark Lathrop[9], Pierre Cau[1,10] and Pierre Szepetowski[1,*]

[1]INSERM UMR491 and [2]INSERM U559, Université de la Méditerranée, 13385 Marseille, France, [3]Clinique Neurologique, [4]Département de Neuropédiatrie and [5]Laboratoire de Cytogénétique, Hôpitaux Universitaires, 67091 Strasbourg, France, [6]Department of Medicine, The University of Melbourne, 3081 Australia, [7]IMVT, IBDM, 13288 Marseille, France, [8]CNRS UMR7004, 67085 Strasbourg, France, [9]Centre National de Génotypage (CNG), 91057 Evry, France, [10]Laboratoire de Biologie Cellulaire, AP-HM, 13385 Marseille, France, [11]Département de Génétique Médicale, AP-HM, 13385 Marseille, France and [12]Department of Neuropediatrics, University of Giessen, Giessen D-35385, Germany and [13]Netherlands Brain Bank, Amsterdam 1105 AZ, The Netherlands

Received November 11, 2005; Revised January 16, 2006; Accepted February 15, 2006

The rolandic and sylvian fissures divide the human cerebral hemispheres and the adjacent areas participate in speech processing. The relationship of rolandic (sylvian) seizure disorders with speech and cognitive impairments is well known, albeit poorly understood. We have identified the Xq22 gene *SRPX2* as being responsible for rolandic seizures (RSs) associated with oral and speech dyspraxia and mental retardation (MR). SRPX2 is a secreted sushi-repeat containing protein expressed in neurons of the human adult brain, including the rolandic area. The disease-causing mutation (N327S) resulted in gain-of-glycosylation of the secreted mutant protein. A second mutation (Y72S) was identified within the first sushi domain of SRPX2 in a male with RSs and bilateral perisylvian polymicrogyria and his female relatives with mild MR or unaffected carrier status. In cultured cells, both mutations were associated with altered patterns of intracellular processing, suggesting protein misfolding. In the murine brain, Srpx2 protein expression appeared in neurons at birth. The involvement of SRPX2 in these disorders suggests an important role for SRPX2 in the perisylvian region critical for language and cognitive development.

INTRODUCTION

Speech and language may co-occur with epilepsy but relationship is poorly understood. The speech centers in the human brain are associated with the two major cerebral fissures, the rolandic and sylvian sulci. Seizure disorders localized to this region may be associated with speech disorders (1,2). Acquired epileptic aphasia of the Landau-Kleffner syndrome (MIM 245570) (3) may represent the severe end of a clinical spectrum comprising the continuous spike-and-wave discharges during slow-sleep syndrome (CSWS) at one end and rolandic (sylvian) epilepsy (RE) at the benign end. RE, or benign focal epilepsy with centro-temporal spikes (BECTS; MIM 117100), represents 8–23% of epilepsies in children <16 years of age with a prevalence of more than one per 1000 and a male to female ratio of 3/2 (4). It is

*To whom correspondence should be addressed at: INSERM UMR491, 'Genetics of Human Epilepsies' Group, Faculté de Médecine de la Timone, 27 Bd J Moulin, 13385 Marseille Cedex 5, France. Tel: +33 491324386; Fax: +33 491804319; Email: szepetowski@medecine.univ-mrs.fr

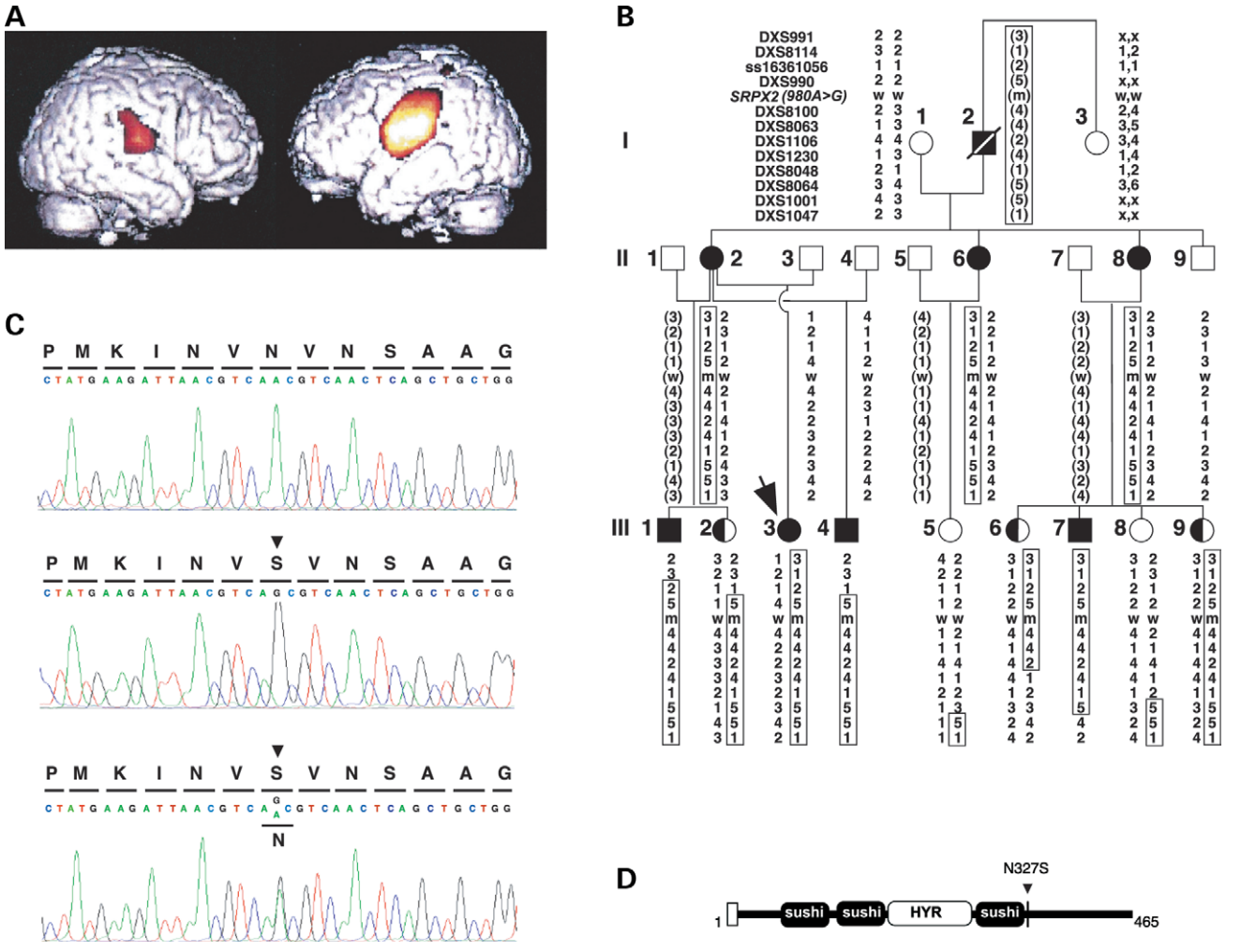

Figure 1. Clinical and genetic data on the French family. (**A**) Fluorodeoxyglucose-positron emission tomography (FDG-PET scan). SPM99 data of FDG-PET scan performed in patient III.3 at age 10 showed bilateral perisylvian hypermetabolism maximum on the left side. (**B**) Chromosome Xq21–q22 haplotypes in the French family. Full-blackened symbols represent affected subjects with RE, MR and OSD. Half-filled blackened symbols represent patients with MR and OSD. White symbols represent unaffected individuals. The arrow indicates the proband. m, mutant allele; w, wild-type allele. Framed numbers represent segregation of the disease haplotype within the family. Non-framed numbers represent non-disease haplotypes. Haplotypes in brackets were inferred from genotyping data obtained in the sibs. Marker genotypes are shown from centromere to q terminus. (**C**) 980A>G transition within exon 9 of *SRPX2*. The nucleotide sequences and translations are shown above the direct sequencing trace from PCR-amplified exon 9. (Top) Section of wild-type sequence in one healthy individual. (Middle) Section of sequence with the mutation (arrowhead) in one affected male (III.1). (Bottom) Section of sequence with the mutation (arrowhead) in one affected female (III.3). (**D**) Schematic representation of the SRPX2 protein. The different domains of the protein are indicated. White box at the N-terminus indicates the signal peptide. (Vertical bar) The N327S mutation (arrowhead) creates an N-glycosylation consensus site (N-X-S/T).

defined by brief and hemi-corporeal motor seizures, frequently associated with somato-sensory symptoms and occurring mainly during sleep. Most idiopathic REs do not follow a Mendelian mode of inheritance (5) and genetic influences have been recently questioned (6).

Idiopathic rolandic seizures (RSs) occur during a period of significant brain maturation. During this time, dysfunction of neural network activities such as focal discharges may be associated with specific developmental disabilities. Subtle specific cognitive impairments of language, visuo-spatial abilities or attention, are observed in children with RS (1,7–10). An autosomal dominant syndrome of RS with oral and speech dyspraxia (OSD; MIM 602081) and cognitive impairment has been reported (ADRESD; MIM 601085) (11).

We investigated a French family (Fig. 1) that had RS with OSD and a variable degree of mental retardation (MR), similar to ADRESD, although the disorder did not follow autosomal inheritance. After careful phenotyping and successful linkage to Xq, mutation screening led to the identification of the disease-causing gene, *SRPX2*. The mutation led to a gain-of-glycosylation of the protein. Another mutation in *SRPX2* was then found in a male patient with epilepsy associated with a malformation of the perisylvian area and in his female relatives with cognitive impairment.

RESULTS

Clinical data on the French family with OSD, RS and MR (Fig. 1)

The proband (III.3) is a right-handed girl, born following a normal pregnancy. At 2 1/2 years of age, language was still

lacking when diurnal and nocturnal RS started. At age 10, she was referred to the Department of Neurology in Strasbourg, where neurological examination showed oro-facial dyspraxia and severe speech delay (Supplementary Material, Video 1). Neuropsychological assessment showed severe oral and finger dyspraxia and impaired verbal comprehension associated with inattention. She was unable to perform any verbal or non-verbal subtest of WPPSI. At age 15, WISC-R provided a full-scale intelligence quotient (IQ) of 40, a verbal IQ (VIQ) of 46 and a performance IQ (PIQ) of 46 (Supplementary Material, Table S1). She had never learned written language. Follow-up awake electro-encephalogram (EEG) recordings showed multiple asynchronous interictal diphasic sharp waves predominant over the left fronto-temporal region (Supplementary Material, Fig. S1). Paroxysms increased during sleep and spread contralaterally. From age 10, she was treated with multiple anti-epileptic drugs. Cytogenetic analysis and fragile X DNA testing were normal. Although magnetic resonance imaging (MRI) showed normal, [^{18}F]fluorodeoxyglucose-positron emission tomography (FDG-PET) performed at age 10 showed bilateral perisylvian hypermetabolism maximal on the left side (Fig. 1). The clinical data on all patients of the French family are summarized in Supplementary Material, Table S1. None of the patients had any dysmorphic features. In addition to III.3, six relatives (II.2, II.6, II.8, III.1, III.4 and III.7) of the proband had focal seizures with the typical clinical features of RS. The electro-encephalographic hallmark of RS (centro-temporal spikes that tend to occur in clusters and are strongly activated during sleep) was detected during the active phase of the epileptic seizures. Multiple epileptic foci were found in three patients (III.3, III.4 and III.7). Two (III.4 and III.7) also had multiple asynchronous interictal EEG abnormalities represented by diphasic sharp waves associated with focal slowing. All patients had OSD with variable impairment of oro-facial motility and of verbal and fine motor abilities (Supplementary Material, Table S1; Supplementary Material, Video 1). IQ was below the normal range in all patients except for II.6 who could not be evaluated. Significant discrepancy between VIQ and PIQ was found in two patients with RS (II.2 and III.1) and in one patient without RS (III.2). Among the three patients without RS, one (III.6) had more severe oro-facial and fine motor impairment. The three patients (III.3, III.4 and III.7) with multiple epileptic foci also had lower full-scale IQs without significant VIQ/PIQ discrepancy.

Linkage analysis and mutation screen

A whole genome screen was performed, using highly polymorphic markers regularly spaced across the genome with an average interval of 10 cM. Consistent with the absence of any male-to-male transmission of the phenotype, linkage to chromosome Xq was obtained with significant LOD (logarithm of the odds ratio for linkage) scores of 3.01 at a recombination fraction of 0 (Supplementary Material, Table S2). With respect to the ADRESD syndrome (11), X-linkage thus demonstrated genetic heterogeneity of the syndrome of OSD with RS and MR.

The region containing the disease gene spanned ~20 cM at Xq21–q22, between markers ss16361056 and DXS1230. FISH analyses with BACs regularly spaced across this area did not detect any large-scale rearrangement (data not shown). A systematic mutation screen led to the detection of an A to G transition (980A>G) in exon 9 of the *SRPX2* gene (Fig. 1). 980A>G perfectly co-segregated with the phenotype in the family (Fig. 1) and was neither found *in silico* nor in 554 control X-chromosomes from unrelated males and females of Caucasian origin. In all the other known genes and coding transcripts analyzed, only polymorphisms or rare variations also detected *in silico* or in the control population were found (Supplementary Material, Table S3). The SRPX2 protein (465 aminoacids; GenBank NP_055282) contains a signal peptide and three consensus sushi-repeat motifs of approximately 60 aminoacids, each that are mostly found in proteins of the complement system and in various others including members of the selectin family (12). It also displays a hyalin repeat (HYR) domain, which is related to the immunoglobulin (Ig)-like fold (13). Previous experiments showed that SRPX2 was secreted (14). The mutated aminoacid (N327S) is conserved among known or predicted SRPX2 proteins in *Homo sapiens*, *Pan troglodytes*, *Mus musculus*, *Rattus norvegicus*, *Canis familiaris* (all with MKINVN$_{327}$VNSAA) and *Xenopus laevis* (MLINVN$_{327}$VNSAG). RT–PCR experiments performed with RNAs extracted from fibroblasts of patient III.1 did not reveal any splicing abnormality (data not shown), but *in silico* search predicted a putative N-glycosylation consensus site (N-X-S/T) that was created by the mutation eight aminoacids downstream from the third sushi domain (Fig. 1). Extra oligosaccharides usually modify the folding of secreted proteins and their interactions with other proteins, and several disease-causing mutations leading to the formation of N-glycosylation sites have been reported (15,16). Indeed, the importance of gain-of-glycosylation mutations in human diseases has very recently been re-emphasized (17).

N327S leads to partial gain-of-N-glycosylation of the mutant SRPX2 protein

To confirm the utilization of this N-glycosylation site, an analysis by sodium dodecyl sulfate–polyacrylamide gel electrophoresis (SDS–PAGE) of wild-type and mutant N327S SRPX2 proteins synthesized by transfected CHO cells and immunoprecipitated with anti-SRPX2 antibodies was performed. Cells were pulse-labeled with [^{35}S]methionine and then chased at various intervals of time with an excess of unlabeled methionine. In both the intracellular and extracellular fractions, mutant N327S SRPX2-DsRed fusion proteins were detected with increased (79 kDa) molecular weight (MW) when compared with their wild-type counterpart (77 kDa, as expected) (Fig. 2). Deglycosylation with PNGase F resulted in a reduction in MW of the 79 kDa mutant protein, which then co-migrated with the wild-type protein (Fig. 2). These data confirmed that the observed migratory difference between these proteins was due to a difference in their N-glycosylation status. In the two fractions, the co-detection of mutant SRPX2 protein of the same MW (77 kDa) as the wild-type protein (Fig. 2) showed that a

subset of the mutant SRPX2 protein was not modified by N-linked glycosylation. Partial uses of N-glycosylation sites have already been described in pathogenic conditions (18,19) and the presence of V at the X position of the N-X-S sequon has actually been associated with partial N-glycosylation (20).

N327S results in altered intracellular processing of SRPX2

Gains of N-glycosylation usually lead to misfolding of secreted proteins. Retention of the mutant SRPX2 fusion protein was indeed detected within the endoplasmic reticulum of a subset of transfected CHO cells (5–10%), as shown by co-localization with calreticulin (Fig. 3). In contrast, the wild-type fusion protein displayed in all transfected cells a much weaker and diffuse cytoplasmic fluorescent pattern. Similar data were obtained when cultured cortical neurons from murine embryos were transfected (Fig. 3). In a subset of patient fibroblasts, retention of the native mutant SRPX2 protein within the endoplasmic reticulum was also detected by co-immunofluorescence staining with anti-SRPX2 and anti-calreticulin antibodies, whereas no such abnormal retention of wild-type SRPX2 was ever observed in the control fibroblasts (Fig. 3). Moreover, mutant SRPX2 and ubiquitin co-localized in patient fibroblasts but never in control fibroblasts (Fig. 3), indicating that a fraction of the mutant protein is probably ubiquitinylated. Altogether, these data demonstrate altered intracellular processing and hence suggest misfolding of the mutant SRPX2 protein.

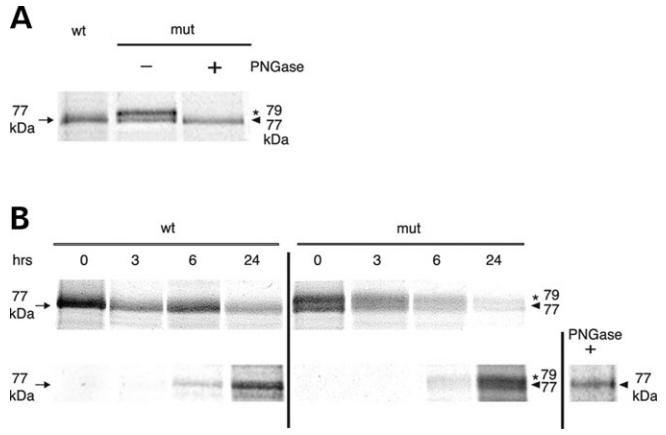

Figure 2. Mutant (N327S) SRPX2 protein is N-glycosylated. CHO cells were transfected with pSRPX2wt-DsRed or pSRPX2mut327-DsRed and pulse-labeled with [^{35}S]methionine. Immunoprecipitated SRPX2 fusion proteins were submitted to SDS–PAGE. (**A**) Enzymatic deglycosylation of the mutant N327S (mut) protein in the intracellular fraction leads to a reduction in MW of the 79 kDa mutant fragment, which then co-migrates with the wild-type (wt) fragment. (+) PNGase F; (−) no PNGase F. The arrows indicate the 77 kDa fragment corresponding to the wild-type SRPX2 protein, the arrowheads indicate the 77 kDa fragment corresponding to the non-N-glycosylated form of the mutant N327S SRPX2 protein and the asterisks indicate the 79 kDa fragment corresponding to the N-glycosylated form of the mutant N327S SRPX2 protein. (**B**) Wild-type (wt; left panel) and mutant N327S (mut; right panel) SRPX2 fusion proteins were recovered after exposure to an excess of unlabeled methionine for various length of time (0, 3, 6 and 24 h). (Top) Intracellular fraction. (Bottom) Extracellular fraction. Enzymatic deglycosylation (PNGase +) of mutant N327S SRPX2 in the extracellular fraction confirmed the data obtained with the intracellular fraction in (A).

SRPX2 is mutated in a patient with bilateral perisylvian polymicrogyria

Bilateral perisylvian polymicrogyria (BPP; MIM 300388) is the most common form of polymicrogyria and X-linked inheritance occurs in some families (21). BPP is characterized by an excess of small gyri and abnormal cortical lamination in the perisylvian area. Difficulties with speech, epilepsy, mild MR and perisylvian abnormalities on imaging studies are classically described in BPP and reflect the inter-relationship of RS and speech disorders and their co-localization to rolandic and perisylvian cortex (1,2). In order to test the possible involvement of *SRPX2*, a first series of 12 patients with BPP was screened. In particular, male patient T2472-1 had bilateral posterior perisylvian polymicrogyria, more severe on the left and extending back to involve the parieto-occipital regions (Fig. 4). He presented at 12 years with focal seizures beginning with numbness of the fingers of the right hand and leg and a sudden fall. Other attacks began with twitching of the right side of his mouth, drooling and loss of awareness. Pregnancy and perinatal history were unremarkable. He walked at 19 months and was a clumsy child. He was left-handed. Neurological examination revealed clonus at both knees and generalized hyperreflexia with an equivocal right plantar response. Neuropsychological evaluation at 15 years showed low average to average intellect (full-scale IQ 86, VIQ 84 and PIQ 92) with weakness in mathematical ability. His EEG showed left centro-temporal epileptiform activity with a rolandic horizontal dipole. Karyotype was normal. He responded initially to carbamazepine but later required polytherapy. Two of his maternal aunts, T2472-4 and T2472-5, had mild MR and his mother (T2472-2) and another aunt (T2472-7) were of normal

Figure 3. Characterization of wild-type and mutant (N327S) SRPX2 proteins in cultured cells. (**A**) Partial retention of the N327S mutant SRPX2-DsRed fusion protein in the endoplasmic reticulum of transfected CHO cells: mutant SRPX2 protein and calreticulin co-localize, as visualized by confocal microscopy. *Left panel*: (Control) CHO cells transfected with non-recombinant pDsRed1-N1 [DsRed (tag) control protein]. *Right panel*: CHO cells were transfected with pSRPX2wt-DsRed (top, wt) or pSRPX2mut327-DsRed (bottom, N327S) constructs. The endoplasmic reticulum was immunostained using anti-calreticulin antibodies. (**B**) Partial retention of the N327S mutant SRPX2-DsRed fusion protein in the endoplasmic reticulum of transfected cortical neurons: mutant SRPX2 protein and calreticulin co-localize, as visualized by confocal microscopy. *Left panel*: (Control) Neurons transfected with non-recombinant pDsRed1-N1 [DsRed (tag) control protein]. *Right panel*: Cortical neurons were transfected with pSRPX2wt-DsRed (top, wt) or pSRPX2mut327-DsRed (bottom, N327S) constructs. The endoplasmic reticulum was immunostained using anti-calreticulin antibodies. (**C**) Partial retention of the N327S mutant SRPX2 endogenous protein in the endoplasmic reticulum of patient fibroblasts. (Top) Control fibroblasts. (Bottom) Patient III.4 fibroblasts. Fibroblasts were processed for immunofluorescence microscopy using DAPI (4′,6-diamidino-2-phenylindole) and antibodies for SRPX2 and calreticulin, as indicated. (**D**) Ubiquitinylation of the N327S mutant SRPX2 endogenous protein in fibroblasts of patient III.4. *Top*: Control fibroblasts. *Bottom*: Patient fibroblasts. Very weak or no SRPX2 and ubiquitin staining was detected in control fibroblasts. Fibroblasts were processed for immunofluorescence microscopy using DAPI and antibodies for SRPX2 and ubiquitin, as indicated.

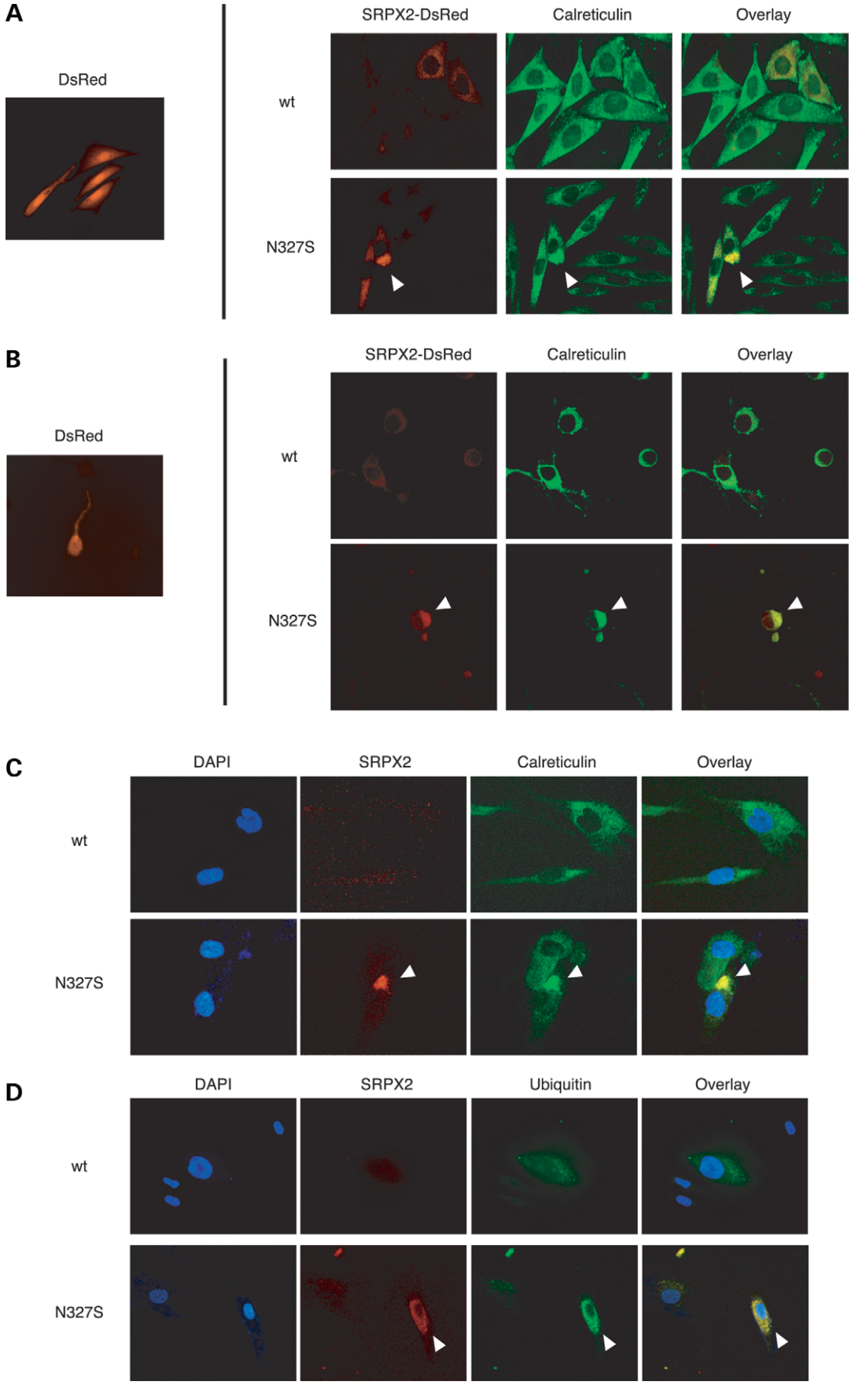

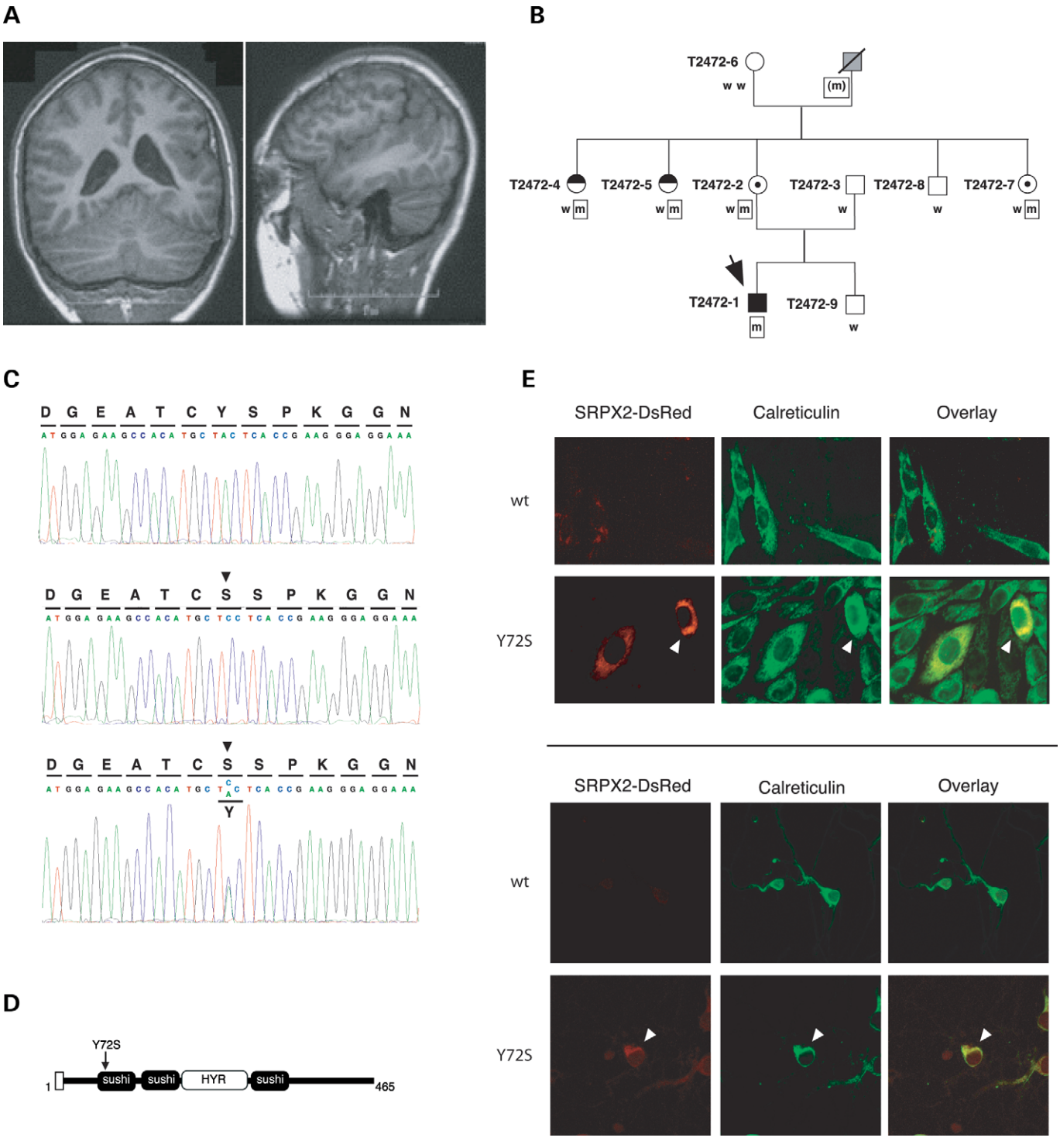

Figure 4. Data on the Australian family with BPP. (**A**) MRI of patient T2472-1 showing BPP. *Left*: Coronal T1 weighted image. *Right*: Left parasagittal image. (**B**) Segregation of the 215A>C transversion within exon 4 of *SRPX2* in the Australian family with BPP or mild MR. Full-blackened square represents the patient affected with BPP. Half-filled blackened circles represent women with mild MR. White symbols represent unaffected individuals. Dotted circle represents the unaffected female carriers. Gray square indicates unknown clinical status. The arrow indicates the proband. m, mutant allele; w, wild-type allele. (**C**) 215A>C transversion within exon 4 of *SRPX2*. The nucleotide sequences and translations are shown above the direct sequencing trace from PCR-amplified exon 4. *Top*: Section of wild-type sequence in one healthy individual. *Middle*: Section of sequence with the mutation (arrowhead) in the patient with BPP (T2472-1). *Bottom*: Section of sequence with the mutation (arrowhead) in a female (T2472-4) with mild MR. (**D**) Schematic representation of the SRPX2 protein. The different domains of the protein are indicated. White box at the N-terminus indicates the signal peptide. The arrow indicates the Y72S mutation within the first sushi domain of SRPX2. (**E**) Partial retention of the Y72S mutant SRPX2-DsRed fusion protein in the endoplasmic reticulum of transfected CHO cells (top) or cortical neurons (bottom): mutant SRPX2 protein and calreticulin co-localize, as visualized by confocal microscopy. CHO cells and cortical neurons were transfected with non-recombinant pDsRed1-N1 (Fig. 3A and B) and with pSRPX2wt-DsRed (top, wt) or pSRPX2mut72-DsRed (bottom, Y72S) constructs. The endoplasmic reticulum was immunostained using anti-calreticulin antibodies.

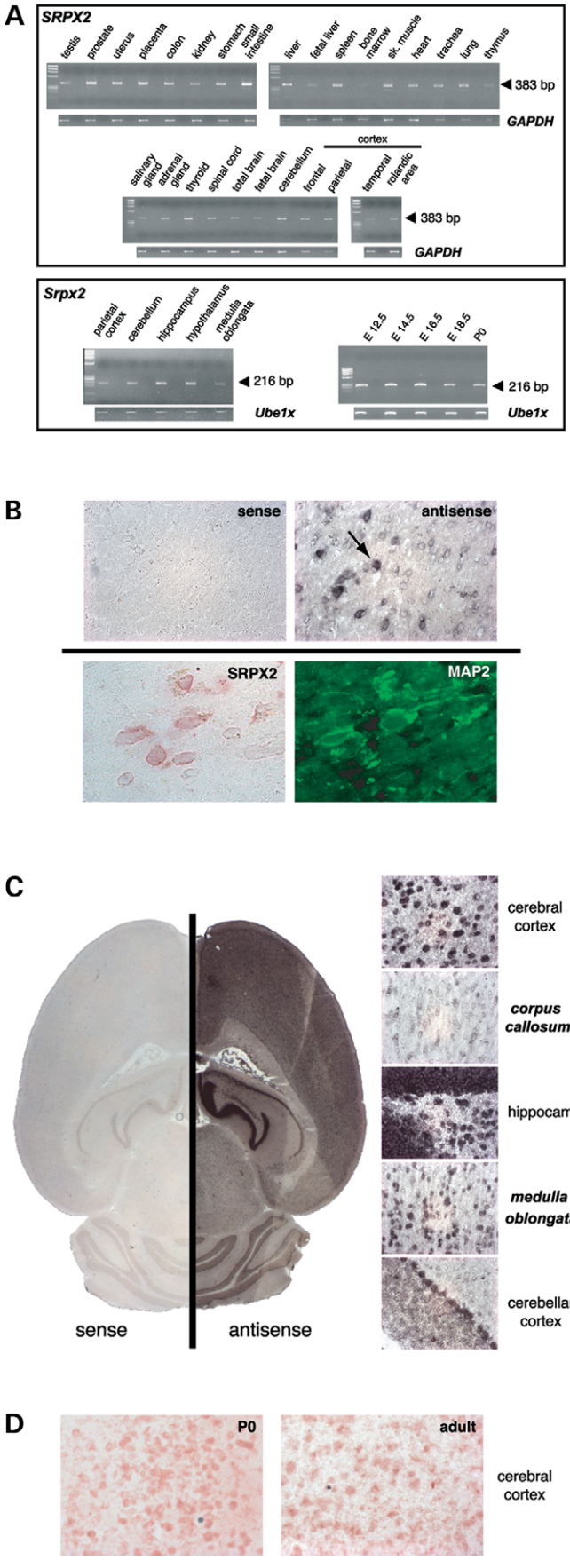

Figure 5. Spatio-temporal expression studies. (**A**) RT–PCR experiments in human (top) and mouse (bottom) tissues. The sizes of PCR fragments in human (*SRPX2*) and mouse (*Srpx2*) are indicated by an arrowhead. *GAPDH*, human expression control. *Ube1x*, mouse expression control; E12.5–14.5, total embryos; E16.5–18.5, embryonic brains; P0, brain at birth. (**B**) Localization of SRPX2 mRNAs (top panel) and protein (bottom panel) in the human rolandic area. (Top panel) *In situ* hybridization experiments. *SRPX2* antisense riboprobe but not control sense probe labeled neuron perikarya. A labeled neuron is indicated by an arrow. (Bottom panel) Immunodetection of SRPX2 and MAP2. SRPX2 was restricted to neuron perikarya, whereas MAP2 also stained dendrites. (**C**) Localization of *Srpx2* mRNAs in the adult mouse brain. *In situ* hybridization experiments using the antisense riboprobe (right panel) labeled neuron perikarya from cerebral and cerebellar cortex, from *medulla oblongata* as well as dentate gyrus and pyramidal cells from the hippocampus. Glial cells from *corpus callosum* remained unlabeled. (Left panel) Control sense riboprobe. (**D**) Immunodetection of murine Srpx2 protein in neurons of the cerebral cortex. *Left panel*: Brain at birth (P0). *Right panel*: Adult brain.

intellect. MRI brain scans on all four women and the proband's brother did not show a cortical malformation (data not shown).

A mutation (215A>C) was detected in exon 4 of the *SRPX2* gene in patient T2472-1 (Fig. 4). 215A>C gave rise to a missense mutation (Y72S) and was neither found *in silico* nor in 624 control X-chromosomes from unrelated males and females of same (Caucasian) origin. 215A>C was also found in the unaffected mother and one unaffected aunt of T2472-1 as well as in the two maternal aunts with mild MR and no MRI abnormality (Fig. 4). As for N327S, the mutated aminoacid (Y72S) was conserved in *H. sapiens*, *P. troglodytes*, *M. musculus*, *R. norvegicus*, *C. familiaris* and *X. laevis*. Y72S occurs within the first sushi domain of SRPX2 in the immediate vicinity of a cysteine residue (C71) that is predicted to participate in the disulfide bond of the sushi domain. Missense mutations situated nearby cysteine residues involved in disulfide bridging may have a dramatic impact on protein folding (22,23) and disulfide bridging is a crucial determinant in the structure of sushi domains (12). Indeed, the orientation in space of a sushi module is likely to be critical for function of sushi-containing proteins (24). As in the case of N327S, partial retention of the Y72S mutant SRPX2 fusion protein in CHO cells and in cortical neurons, but not of the wild-type protein, suggested misfolding (Fig. 4).

Expression of SRPX2 transcripts and protein in the human and murine brain

We next analyzed the expression pattern of *SRPX2* in human and mouse tissues. Expression of *SRPX2* was detected *in silico* (Unigene Hs.306339) and by RT–PCR experiments in most human tissues tested including the fetal and adult brain (Fig. 5A). *In situ* hybridization experiments performed on human autopsy samples corresponding to the rolandic area showed that *SRPX2* was apparently expressed in neurons only (Fig. 5B). Immunohistochemistry experiments confirmed that the human SRPX2 protein was expressed in neuron perikarya of the rolandic area (Fig. 5B). In mouse, RT–PCR as well as *in situ* hybridization and immunohistochemistry experiments detected Srpx2 mRNA and protein in several areas of the adult brain (Fig. 5). In mouse

embryos, *Srpx2* expression was detected *in silico* (Unigene Mm.263553) and by RT–PCR at various stages (E12.5–14.5–16.5–18.5), in the brain particularly (Fig. 5A). Immunohistochemistry experiments demonstrated expression of the Srpx2 protein in neurons of the murine brain at birth (P0) (Fig. 5D) but not at any previous embryonic stage tested (data not shown). RSs occur during a period strongly correlated with brain maturation and speech processing may partly depend on specific stages of perinatal and postnatal maturation of the cerebral cortex, when brain growth, circuit organization and many other crucial modifications occur in primates (25).

DISCUSSION

We show here that the Xq22 *SRPX2* gene is mutated in a French family presenting with RS, OSD and a variable degree of MR. The N327S mutation led to gain-of-glycosylation of the mutant SRPX2 protein. Our data thus confirm the importance and the pathogenic role of such types of mutations in human disease (17). Gains of oligosaccharides are usually associated with modifications in the folding of secreted proteins and in their interactions with other proteins. As shown by the specific observation of altered patterns of SRPX2 processing inside a subset of cells, the N-glycosylation of mutant SRPX2 is also likely to be associated with conformational changes, which in turn would modify the specific interactions and functioning of the secreted mutant SRPX2 protein outside the cells. In the French family studied here, the phenotypes in males and females displayed quite similar levels of severity despite X-linkage. This unusual feature is likely to rely on the partial use of the mutant N-glycosylation site, leading to the secretion of both N-glycosylated and non-N-glycosylated SRPX2 proteins, not only in females but also in males. The possibility of SRPX2 dimerization must be considered, as already shown for other sushi-containing proteins (26,27). This would fit well with a dominant-negative effect. Haploinsufficiency of SRPX2 is an alternative hypothesis, with subtle dosage effects between wild-type SRPX2, non-N-glycosylated mutant SRPX2 and N-glycosylated mutant SRPX2 proteins. Moreover, inter-individual variations in the efficacy and rates of N-glycosylation cannot be excluded. Alternatively, gain-of-glycosylation leading to gain-of-function has also been described (15); the secreted mutant SRPX2 protein may then exert its effects on more than the classical 50% of SRPX2-producing cells in females. Last but not least, severe skewed X-inactivation patterns were detected in the lymphocytes of two affected women, II.6 and III.3 (Supplementary Material, Fig. S2). About 90% of the X-chromosomes bearing the disease haplotype were inactivated in these two women, although they did not have a milder phenotype (both had RE and OSD). Paradoxical patterns of skewed inactivation have already been observed in women severely affected with the X-linked dominant otopalatodigital disorders (MIM 300017) and displaying mutations in the *FLNA* gene (28). Moreover, a reverse pattern of skewed inactivation was obtained (compared with that seen in the lymphocytes) in the fibroblasts of III.3 (fibroblasts were not available for patient II.6), as 80% of her X-chromosomes bearing the wild-type haplotype were inactivated (Supplementary Material, Fig. S2). Such a skewed pattern of X-inactivation in fibroblasts was thus consistent with the severe phenotype displayed by patient III.3 and could be similar in brain tissue.

Another disease-causing mutation in the first sushi domain of SRPX2 was identified in a patient with seizures of the rolandic area and BPP and in his female relatives with mild MR only. As described for other genes such as *ARX* (29), the pleiotropy in the phenotypes associated with *SRPX2* mutations may reflect a continuous spectrum of disorders from malformations of cortical development (polymicrogyria) to epilepsy, MR and speech impairment. Whether SRPX2 may participate in more common forms of such disorders seems unlikely, as no mutations were detected in 81 sporadic or familial idiopathic REs (Materials and Methods). This is consistent with the genetic complexity and heterogeneity (30) or even with the weak genetic influence reported for most idiopathic RE (6) and may suggest the absence of a direct link between idiopathic RE and the RS occurring in complex syndromes. Similarly, no further mutations were found in an additional series of patients with BPP (Materials and Methods); this is consistent with both the high level of genetic heterogeneity and the existence of non-genetic forms of BPP (21).

The involvement of sushi-repeat proteins in human brain disorders had not been demonstrated so far. On the one hand, sushi domains are found in a number of proteins from vertebrates and invertebrates and function as protein-binding modules (12,31,32). Sushi (12) and HYR domains (13) appear to be involved in cell adhesion processes and the hikaru genki protein, which also contains several sushi modules and one Ig-like domain, is secreted at synaptic clefts and is involved in the development of the central nervous system in *Drosophila melanogaster* (33). On the other hand, as sushi domains are frequently found in complement binding proteins (12), SRPX2 may interact with components of the complement system in brain tissue. Interestingly, a role of the complement system in normal brain functioning and in brain pathologies, including the epilepsies, has been proposed (34–36).

In contrast with brain imaging data, very little is known at the molecular level on brain areas controlling articulation (37). In addition to rolandic/sylvian epileptic seizures, difficulties in coordinating and sequencing the oral-motor movements or perisylvian polymicrogyria may be encountered in patients with *SRPX2* mutations. This gene may thus play an important role in the functioning and development of the rolandic and perisylvian regions. Mutations within *FOXP2* also cause OSD (38) and the *FOXP2* human mRNA is expressed in the perisylvian areas; however, the widespread expression of the murine and human *FOXP2* (39) makes it difficult to draw any specific conclusion. Interestingly, the lack of detection of Srpx2 expression during murine embryogenesis may suggest a specific role for SRPX2 in human brain development, of the rolandic and sylvian areas particularly. *SRPX2* mutations also add to the list of X-linked genetic defects that cause MR. The data reported here thus open new and exciting insights in the pathophysiology and inter-relationship of RE, speech impairment and MR.

MATERIAL AND METHODS

Subjects

Two patients from the French family (Fig. 1), a 10-year-old girl (III.3) and her half-brother aged 4 (III.4), were referred to the Neurology Department at Strasbourg University Hospital. They both had a history of epileptic seizures with speech impairment. Familial history of epilepsy was detected as several relatives were reported with similar seizures. Medical records were collected from all family members. Interictal and ictal EEG recordings were obtained with diurnal and nocturnal video-EEG monitoring performed with 20 scalp electrodes positioned according to the international 10-20 system. The subjects underwent neuropsychological evaluation consisting of testing handedness, verbal, visual, spatial and mental abilities. Two patients (II.6 and III.4; Supplementary Material, Table S1) could not perform all tests because of behavioral issues during the evaluation. Handedness was evaluated using the appropriate questionnaire (40). IQ was measured by using either the Wechsler Adult Intelligence Scale Revised (WAIS-R) (41) or the Wechsler Intelligence Scale for Children Revised (WISC-R) (42), or the Wechsler Preschool and Primary Scale of Intelligence Revised (WPPSI-R) (43) tests, depending on the age. Raven's progressive matrices were used to measure non-verbal intelligence in three subjects (II.8, III.6 and III.9). Semantic and phonological fluency as well as word repetition were performed to evaluate lexical processing. Verbal and non-verbal oro-facial motility was assessed using the subtests of the Boston diagnosis of aphasia examination (44). Neuroimaging data (computed tomography/MRI) were obtained from five affected individuals (II.2, III.1, III.3, III.4 and III.7). Metabolic brain studies with FDG-PET were performed in patient III.3 at age 10 and analyzed using the SPM99 image analysis software (45).

In addition to this French family, other patients with related disorders were also collected. The phenotypes included sporadic or familial RE (81 unrelated patients), the syndrome of continuous spike and wave during slow sleep (CSWS; nine unrelated patients), typical acquired epileptiform aphasia (Landau-Kleffner syndrome; MIM 245570) or related epilepsy–aphasia syndromes (17 unrelated patients), unilateral (three unrelated patients) or BPP [a first series of 12 unrelated patients, including patient T2472-1, and a second series of 14 unrelated patients, including one patient with LKS and BPP (46)], speech impairment with or without epilepsy (four unrelated families) and a heterogeneous group of 42 patients with various types of complex, developmental (schizencephaly, lissencephaly, microcephaly, etc.) and/or cognitive disorders. All patients had given informed consent for collection of blood samples and were subjected to careful clinical, EEG and imaging examinations.

Linkage studies on the family with OSD, RE and MR

All family members gave informed consent for collection of blood samples, as recommended by the appropriate Ethics Committee. High-molecular-weight genomic DNA was isolated from whole blood using the Nucleon® kit (Amersham Biosciences). Highly polymorphic microsatellite markers were analyzed by PCR amplification of 20–40 ng of genomic DNA in 10–50 μl reactions with 50–335 nM of each primer, 1–3 mM $MgCl_2$, 200–250 μM each nucleotide and 0.4–0.5 U of *Taq* Polymerase (AmpliTaq Gold™). Forward primers were labeled at the 5′ terminus with a fluorescent dye (Fam-Tet/Ned-Hex or D2-D3-D4, depending on the sequencer). Fluorescent PCR products were analyzed either on a MegaBACE™ 1000 Sequencer (Amersham Biosciences) or on a CEQ-8000™ Sequencer (Beckman Coulter), using the appropriate softwares. Linkage analyses were performed under the assumption of an autosomal or X-linked dominant mode of inheritance with penetrance at 1.0, frequency of the disease at 0.0001, phenocopy rate at 0 and equal allele frequencies, by the use of MLINK in the LINKAGE computer package (47).

Mutation screening

The whole coding sequences of the known genes and transcripts analyzed within the region of interest were screened for mutations by direct sequencing of each exon and the surrounding intronic sequences, using DNA from patient III.1 (Supplementary Material, Table S3). Both strands of each corresponding PCR product were sequenced with an ABI3700 DNA Analyzer™ (Applied Biosystems) or with a CEQ-8000™ Sequencer (Beckman Coulter). Sequencing data were analyzed with the Genalys 3.0 software. The *SRPX2* gene was screened in genomic DNAs after PCR amplification of each exon, using the following primers: exon 1: forward 5′-gcttaagccagcctctgtgt and reverse 5′-tgggtctccttatcccc ttc; exon 2: forward 5′-gggaggaaaagggaccataa and reverse 5′-agtctaactcttccttctccaagtc; exon 3: forward 5′-agttggatgaga gggggaag and reverse 5′-aatcacagcccctgattcc; exon 4: forward 5′-tgtcttttcaccaacaccaca and reverse 5′-tccgggcat ataccctcag; exon 5: forward 5′-tctgatgtttctccctgtgct and reverse 5′-ggaatgccttctgtggtgag; exons 6 and 7: forward 5′-gtgtgtggcattgcttcagt and reverse 5′- ggtgggtcagggtagagcag; exon 8: forward 5′-gcaccctcttagcctttcct and reverse 5′-cctgtccatgaggaagatcc; exon 9: forward 5′-atgggagaaacagc cagaga and reverse 5′- tgctgcagagaacaactctga; exon 10: forward 5′-cctttcccacactgcttcat and reverse 5′- aagtttggcag cctccca; exon 11: forward 5′-gtagagcctgtggggatgg and reverse 5′-tgtcaaactcacccacctca.

Generation of constructs

Full-length wild-type and mutant (N327S) human *SRPX2* coding sequences were amplified by RT–PCR from total RNAs of one control individual and of one patient, respectively, using the forward primer 5′-AAAAAAAGCTTA TGGCCAGTCAGCTAACTCA and the reverse primer 5′-A AAAAGGATCCGGCTCGCATATGTCCCTTTGCT. The cDNAs were subcloned into pDsRed1-N1 (Clontech) in order to produce fusion proteins with the tag at the C-terminus. The 215A>C mutation (Y72S) was introduced into the wild-type construct using the XL Quickchange mutagenesis kit (Stratagene). All insert sequences and orientations were confirmed by automated sequencing (Beckman-Coulter).

Cell culture and transfection

CHO cells and human fibroblasts were grown in 5% CO_2 at 37°C in Ham's F-12 nutrient mixture (Life Technologies) supplemented with 2 mM glutamine, 100 U/ml penicillin, 100 μg/ml streptomycin and 10% fetal calf serum. When cells reached 70–80% confluence, they were transfected (CHO cells) or harvested with 0.25% trypsin and 0.05% EDTA in 10 mM sodium phosphate, 0.15 M NaCl, pH 7.4, buffer (PBS) and aliquots of dissociated cells were plated on 100 mm diameter Petri dishes. CHO cells were transiently transfected with wild-type (pSRPX2wt-DsRed) or mutant (pSRPX2mut327-DsRed, pSRPX2mut72-DsRed) or non-recombinant (pDsRed1-N1) vector using the Lipofectamine Plus™ reagent (Life Technologies) according to manufacturer's protocol. For primary cultures of mouse cortical neurons, these were isolated from E15 mouse embryos. Briefly, cortices were dissected in calcium and magnesium-free HBSS medium supplemented with glucose (Invitrogen), treated with trypsin (0.05%) for 15′ and dissociated by trituration. Neurons were transfected by electroporation as follows: cells were centrifuged and resuspended in PBS (10^6/ml). About 5×10^5 cells were then mixed with 8 μg of pSRPX2wt-DsRed, pSRPX2mut327-DsRed, pSRPX2mut72-DsRed or pDsRed1-N1 vector in a 4 mm-electroporation cuvette, and three electroporation pulses (270 V and 5 ms) were applied using a BTX electroporator (BTX, San Diego). After electroporation, cells were immediately resuspended in NB medium supplemented with B27 (Invitrogen) and plated on poly-D-lysine (0.01 mg/ml) coated cover slips.

Pulse-chase procedure

Forty-eight hours after transfection with pSRPX2wt-DsRed or pSRPX2mut327-DsRed, CHO cells were starved 30 min in methionine-free DMEM medium (Life Technologies). Cells were then pulse-labeled with [^{35}S]methionine (20 μCi/ml). Pulse medium was removed after 1 h incubation, followed by two quick washes with PBS, and cells were chased in Ham's F-12 medium supplemented with the required amount of FCS at different time intervals. At the end of the chase period, cell-free medium, referred to as the extracellular fraction, was supplemented with Complete Protease Inhibitors (Roche). Cells of each dish were then carefully washed twice in PBS without $CaCl_2$ and $MgCl_2$, harvested by scraping with a rubber policeman in lysis buffer [10 mM HEPES (pH 7.4), 1.5% (v/v) Triton X-100, 200 mM NaCl, 2 mM $CaCl_2$ and 2 mM benzamidine], rapidly cooled at 4°C and sonicated (4 W) for 15 s. Cell debris was then pelleted by centrifugation (10 000*g* for 20 min at 4°C) and the supernatant, referred to as the intracellular fraction, was supplemented with Complete Protease Inhibitors (Roche).

Immunoprecipitation and PAGE

Computer prediction programs were used to identify a potential antigenic site from aminoacids 443–456 (FIDDYLLSNQELTQ) within the SRPX2 protein. The peptide was generated (Millegen, Toulouse) and used to immunize two rabbits. Analysis of the serum from these two hosts by enzyme-linked immunosorbent assay demonstrated that both identified the peptide used for immunization. Antibodies were purified from rabbit crude sera with a protein A-Sepharose column (Amersham) according to manufacturer's protocol. Aliquots (1 ml) of the intracellular and extracellular fractions were incubated overnight at 4°C with 30 μg of specific antibodies against human SRPX2. The antigen–antibody complexes were incubated for 4 h at 4°C under agitation with 10 mg of pre-washed protein A-Sepharose. The antigen–antibody protein A complexes were recovered by centrifugation (10 000*g* for 15 min at 4°C). The final pellet was then washed twice with 25 mM Tris–HCl, pH 7.4, buffer containing 5 mM EDTA and 1% Triton X-100. Non-specifically bound proteins were removed from the protein A-Sepharose beads by washing twice with the same buffer containing 1 M NaCl and twice with this latter buffer plus 0.1% SDS and then twice with 10 mM Tris–HCl, pH 7.4, buffer containing 5 mM EDTA. The immunoprecipitated SRPX2 protein was dissociated from the protein A-Sepharose by heating at 95°C for 5 min in Laemmli's sample buffer. When required, protein *N*-glycosidase treatment was applied. After centrifugation (10 000*g* for 5 min at 20°C), the supernatant was analyzed by electrophoresis on SDS-containing 7% polyacrylamide gels (SDS–PAGE) according to Laemmli's protocol (48). After separation by SDS–PAGE, the polyacrylamide gels were stained for 5 min with Coomassie blue R250 and destained overnight in ethanol/acetic acid/water (2/3/35 by volume). The polyacrylamide gels were then dried for 3 h and autoradiographed (BioMax MS films, Eastman-Kodak).

Protein *N*-glycosidase treatment

Immunoprecipitated SRPX2 proteins of the intracellular or extracellular fractions were denatured in 1X glycoprotein denatured buffer (NEB) at 100°C for 10 min, according to manufacturer's protocol. Denatured proteins were then supplemented with 1X G7 buffer, 1% NP-40 and 2 μl PNGase F (NEB) and were incubated at 37°C for 1 h. Samples were then supplemented with an equal volume of 2× Laemmli buffer, heated at 95°C for 5 min, centrifuged at 10 000*g* for 5 min and analyzed by SDS–PAGE, as described earlier. Identical protocol but with no PNGase F was applied to undigested mutant N327S proteins (Mut− in Fig. 2).

RT–PCRs

Total RNAs from human autopsy brain samples corresponding to the frontal and temporal lobes and to the rolandic area and obtained through the Netherlands Brain Bank (Amsterdam) from two donors were prepared by Trizol extraction, according to manufacturer's protocol (Invitrogen). Total RNAs from other human tissues were obtained commercially (Clontech). Total RNAs from various areas of the adult mouse (C57BL6) brain, from mouse brain at birth and from different embryo stages, were also prepared by Trizol extraction. Reverse transcriptions were performed from total RNA (1 μg) using oligo(dT) primer and the SuperScript II RNase H$^-$ Reverse Transcriptase (Invitrogen), according to manufacturer's protocol. One-twentieth of the reaction product was

used for PCR amplification of 30 cycles with specific primers in a 9700 DNA thermocycler (Applera). RT-primers were as follows: human forward primer 5′-TACCACTGT GATGGCGGTTA (cDNA position 1285–1306) and reverse primer 5′-TTGAAGTAGGAGCGAGTGAGG (cDNA position 1668–1648); murine forward primer 5′-TGCCTATG ACCGAGCCTACA (cDNA position 1000–1019) and reverse primer 5′-CCTGACCACTGTCGACTTGA (cDNA position 1215–1195).

In situ hybridization experiments

Human and mouse brain tissues were frozen with liquid–nitrogen vapors and stored at −80°C until use. A riboprobe for *in situ* hybridization experiments was generated from the 5′-UTR of the human *SRPX2* cDNA by PCR amplification. Primers were IS-F 5′-CTGAGTTCCTCTAATCCCTG and IS-R 5′-CTTTAACATTCCTAGAACGAGTG. Either of the two primers included a 22 bp T7 tail at the 5′ end for the generation of sense or antisense probes, thus resulting in a 222 bp PCR fragment. Antisense and sense cRNA probes were produced and labeled with digoxigenin-11-UTP (Roche) by *in vitro* transcription using T7 RNA polymerase (Promega). This riboprobe was also used to study expression of *Srpx2* in mouse tissues, as it displayed strong homology at the nucleotide level (90% along 140 bp) with the corresponding murine fragment of *Srpx2* and did not match any other murine cDNA sequence in the databases. *In situ* hybridization experiments were performed on serial sections (14 μm with a Microm cryostat) as already described (49). In each experiment, controls included slides hybridized with sense probes and slides without any probes (control for non-specific binding of antibodies). Sections were observed with a microscope (Leica, DMR) and CoolSnap camera.

Immunocyto- and immunohistochemistry experiments

Neurons and CHO cells were transfected as described earlier and fixed with 4% paraformaldehyde for 30 min at room temperature. Non-specific binding was blocked in PBS supplemented with 10% normal goat serum. Following a permeabilization step in a 0.1 M phosphate buffer, pH 7.4, containing 0.5% Triton X-100, cells were incubated with a polyclonal calreticulin antibody (1:100; Stressgen). The secondary antibodies were anti-rabbit antibodies conjugated to Alexa 488 (1:400; Molecular Probes). Cover slips were mounted in Vectashield (Vector). Fibroblasts cultured on cover slips (LabTek I, Dutcher) were fixed with 4% paraformaldehyde for 15 min at room temperature. Following primary antibodies were used: rabbit anti-SRPX2 antibody (1:100), rabbit anti-calreticulin antibody (1:100; Stressgen) and rabbit anti-ubiquitin antibody (1:100; DakoCytomation). Because two rabbit-derived antibodies were used simultaneously, a Zenon rabbit IgG labeling kit was employed (Molecular Probes). SRPX2 antibody was labeled with Zenon Alexa Fluor 594 rabbit IgG labeling reagent and calreticulin or ubiquitin antibodies were labeled with Zenon Alexa Fluor 488 rabbit IgG labeling reagent, according to manufacturer's instructions. Fibroblasts were also counterstained with DAPI (4′,6-diamidino-2-phenylindole).

Immunohistochemistry experiments were performed on serial sections of human adult brain samples prepared as described earlier. The following antibodies were used as primary antibodies: rabbit anti-SRPX2 antibody (1:100) and mouse anti-MAP2 (microtubule-associated protein type 2) antibody (1:100; Sigma). Secondary antibodies were anti-rabbit biotin-SP-conjugated antibodies (1:200; Jackson Laboratories) used with enzyme-conjugated streptavidin (Vector) and anti-mouse antibodies conjugated to Alexa 488 (1:400; Molecular Probes). In each experiment, non-immune IgG (from rabbit or mouse, obtained from Jackson Laboratories) was used as negative controls (data not shown). Cells were counterstained with DAPI (data not shown). Serial sections of mouse adult brain samples were prepared as described earlier. Mouse (C57BL6) embryos at embryonic days 12.5, 14.5, 16.5, 18.5 and newborns (P0) were sacrificed and total bodies (E12.5–16.5) or heads (E18.5 and P0) dipped in 4% paraformaldehyde in PBS (pH 7.4). Next, they were cryoprotected overnight with increasing sucrose concentrations (0.5–20%) in PBS. The bodies or the heads were embedded in Tissue Tek O.C.T. compound (VWR) followed by cryosection at 14 μm. Rabbit anti-SRPX2 antibody (1:100) was used as primary antibody. Secondary antibody was anti-rabbit biotin-SP-conjugated antibody (1:200; Jackson Laboratories) used with enzyme-conjugated streptavidin (Vector).

Images were captured with a fluorescence microscope (Leica, DMR) and CoolSnap camera. Transfected cells were also observed by confocal laser microscopy (Leica TCS SP2 microscope equipped with a ArKr and a HeNe lasers and a 63X planAPOchroma oil immersion objective lens).

URLs

We used the following websites for genes, markers, sequence alignment and protein domain prediction: golden path sequence assembly (http://genome.ucsc.edu/), dbSNP, BLAST, OMIM, Unigene and GenBank at NCBI (http://www.ncbi.nlm.nih.gov/), NetNglyc server (http://www.cbs.dtu.dk/services/NetNGlyc/), Genalys 3.0 software (http://software.cng.fr/docs/genalys.html/), Prosite (http://www.expasy.org/), DIpro 2.0 (http://contact.ics.uci.edu/bridge.html/) and SMART (http://smart.embl-heidelberg.de/). SPM99 image analysis software can be found at http://www.fil.ion.ucl.ac.uk/spm/spm99.html/.

SUPPLEMENTARY MATERIAL

Supplementary Material is available at HMG Online.

ACKNOWLEDGEMENTS

We thank all the family members and patients who participated in this study. Each participant gave informed consent prior to the study, according to the appropriate Ethics Committee. We thank S. Fisher and F. Muscatelli for critical reading of the manuscript and C.A. Walsh for his kind and efficient collaboration. We are grateful to A. Vérine, D. Lombardo, F. Watrin, P. Huppke and P. van Bogaert for their help and contribution and to D. Bisogno and N. Favre for their efficient administrative or technical help. Assistance from the 'Genome

Variation' (GenoVarior) core facilities at Marseille-Nice Génopôle, from IFR Jean Roche, Marseille (confocal microscopy) and from the 'Cell culture and DNA library' at Biological Resource Center (BRC), AP-HM, Marseille was greatly appreciated. P.R. is a recipient of an LFCE (Ligue Française Contre l'Epilepsie)-Novartis fellowship. This study was supported by INSERM, FFRE (Fondation Française pour la Recherche sur l'Epilepsie), GIS—Institut des Maladies Rares, National Health and Medical Research Council of Australia and Bionomics Limited.

Conflict of Interest statement. There is no conflict of interest to disclose.

REFERENCES

1. Deonna, T.W., Roulet, E., Fontan, D. and Marcoz, J.P. (1993) Speech and oromotor deficits of epileptic origin in benign partial epilepsy of childhood with rolandic spikes (BPERS). Relationship of the acquired aphasia–epilepsy syndrome. *Neuropediatrics*, **24**, 83–87.
2. Staden, U., Isaacs, E., Boyd, S.G., Brandl, U. and Neville, B.G. (1998) Language dysfunction in children with rolandic epilepsy. *Neuropediatrics*, **29**, 242–248.
3. Landau, W.M. and Kleffner, F.R. (1957). Syndrome of acquired aphasia with convulsive disorder in children. *Neurology*, **7**, 523–530.
4. Dalla Bernardina, B., Sgrò, V. and Fejerman, N. (2002) Epilepsy with centro-temporal spikes and related syndromes. In Roger J, Bureau, M., Dravet, C., Genton, P., Tassinari, C.A. and Wolf, P. (eds), *Epileptic Syndromes in Infancy, Childhood and Adolescence*. John Libbey, London, pp. 181–202.
5. Doose, H. and Baier, W.K. (1989) Benign partial epilepsy and related conditions: multifactorial pathogenesis with hereditary impairment of brain maturation. *Eur. J. Pediatr.*, **149**, 152–158.
6. Vadlamudi, L., Harvey, A.S., Connellan, M.M., Milne, R.L., Hopper, J.L., Scheffer, I.E. and Berkovic, S.F. (2004) Is benign rolandic epilepsy genetically determined? *Ann. Neurol.*, **56**, 129–132.
7. Metz-Lutz, M.N., Kleitz, C., De Saint Martin, A., Massa, R., Hirsch, E. and Marescaux, C. (1999) Cognitive development in benign focal epilepsies of childhood. *Dev. Neurosci.*, **21**, 182–190.
8. De Saint Martin, A., Petiau, C., Massa, R., Maquet, P., Marescaux, C., Hirsch, E. and Metz-Lutz, M.N. (1999) Idiopathic rolandic epilepsy with 'interictal' facial myoclonia and oromotor deficit: a longitudinal EEG and PET study. *Epilepsia*, **40**, 614–620.
9. Gündüz, E., Demirbilek, V. and Korkmaz, B. (1999) Benign rolandic epilepsy: neuropsychological findings. *Seizure*, **8**, 246–249.
10. Yung, A.W., Park, Y.D., Cohen, M.J. and Garrison, T.N. (2000) Cognitive and behavioral problems in children with centrotemporal spikes. *Pediatr. Neurol.*, **23**, 391–395.
11. Scheffer, I.E., Jones, L., Pozzebon, M., Howell, R.A., Saling, M.M. and Berkovic, S.F. (1995) Autosomal dominant rolandic epilepsy and speech dyspraxia: a new syndrome with anticipation. *Ann. Neurol.*, **38**, 633–642.
12. O'Leary, J.M., Bromek, K., Black, G.M., Uhrinova, S., Schmitz, C., Wang, X., Krych, M., Atkinson, J.P., Uhrin, D. and Barlow, P.N. (2004) Backbone dynamics of complement control protein (CCP) modules reveals mobility in binding surfaces. *Protein Sci.*, **13**, 1238–1250.
13. Callebaut, I., Gilges, D., Vigon, I. and Mornon, J.P. (2000) HYR, an extracellular module involved in cellular adhesion and related to the immunoglobulin-like fold. *Protein Sci.*, **9**, 1382–1390.
14. Kurosawa, H., Goi, K., Inukai, T., Inaba, T., Chang, K.S., Shinjyo, T., Rakestraw, K.M., Naeve, C.W. and Look, A.T. (1999) Two candidate downstream target genes for E2A-HLF. *Blood*, **93**, 321–332.
15. Isordia-Salas, I., Pixley, R.A., Parekh, H., Kunapuli, S.P., Li, F., Stadnicki, A., Lin, Y., Sartor, R.B. and Colman, R.W. (2003) The mutation Ser511Asn leads to N-glycosylation and increases the cleavage of high molecular weight kininogen in rats genetically susceptible to inflammation. *Blood*, **102**, 2835–2842.
16. Brennan, S.O., Borg, J.Y., George, P.M., Soria, C., Soria, J., Caen, J. and Carrell, R.W. (1988) New carbohydrate site in mutant antithrombin (7 Ile–Asn) with decreased heparin affinity. *FEBS Lett.*, **237**, 118–122.
17. Vogt, G., Chapgier, A., Yang, K., Chuzhanova, N., Feinberg, J., Fieschi, C., Boisson-Dupuis, S., Alcais, A., Filipe-Santos, O., Bustamante, J. *et al*. (2005) Gains of glycosylation comprise an unexpectedly large group of pathogenic mutations. *Nat. Genet.*, **37**, 692–700.
18. Huang, X.F. and Shelness, G.S. (1999) Efficient glycosylation site utilization by intracellular apolipoprotein B. Implications for proteasomal degradation. *J. Lipid Res.*, **40**, 2212–2222.
19. Buck, T.M., Eledge, J. and Skach, W.R. (2004) Evidence for stabilization of aquaporin-2 folding mutants by N-linked glycosylation in endoplasmic reticulum. *Am. J. Physiol. Cell Physiol.*, **287**, 1292–1299.
20. Shakin-Eshleman, S.H., Spitalnik, S.L. and Kasturi, L. (1996) The amino acid at the X position of an Asn–X–Ser sequon is an important determinant of N-linked core-glycosylation efficiency. *J. Biol. Chem.*, **271**, 6363–6366.
21. Jansen, A. and Andermann, E. (2005) Genetics of the polymicrogyria syndromes. *J. Med. Genet.*, **42**, 369–378.
22. Lux, A., Gallione, C.J. and Marchuk, D.A. (2000) Expression analysis of endoglin missense and truncation mutations: insights into protein structure and disease mechanisms. *Hum. Mol. Genet.*, **9**, 745–755.
23. Le Gac, G., Dupradeau, F.Y., Mura, C., Jacolot, S., Scotet, V., Esnault, G., Mercier, A.Y., Rochette, J. and Ferec, C. (2003) Phenotypic expression of the C282Y/Q283P compound heterozygosity in HFE and molecular modeling of the Q283P mutation effect. *Blood Cells Mol. Dis.*, **30**, 231–237.
24. Henderson, C.E., Bromek, K., Mullin, N.P., Smith, B.O., Uhrin, D. and Barlow, P.N. (2001) Solution structure and dynamics of the central CCP module pair of a poxvirus complement control protein. *J. Mol. Biol.*, **307**, 323–339.
25. Levitt, P. (2003) Structural and functional maturation of the developing primate brain. *J. Pediatr.*, **143** (Suppl. 4), S35–S45.
26. Lacroix, M., Ebel, C., Kardos, J., Dobo, J., Gal, P., Zavodszky, P., Arlaud, G.J. and Thielens, N.M. (2001) Assembly and enzymatic properties of the catalytic domain of human complement protease C1r. *J. Biol. Chem.*, **276**, 36233–36240.
27. Li, P., Wohland, T., Ho, B. and Ding, J.L. (2004) Perturbation of Lipopolysaccharide (LPS) micelles by Sushi 3 (S3) antimicrobial peptide. The importance of an intermolecular disulfide bond in S3 dimer for binding, disruption, and neutralization of LPS. *J. Biol. Chem.*, **279**, 50150–50156.
28. Robertson, S.P., Twigg, S.R., Sutherland-Smith, A.J., Biancalana, V., Gorlin, R.J., Horn, D., Kenwrick, S.J., Kim, C.A., Morava, E., Newbury-Ecob, R. *et al*. (2003) Localized mutations in the gene encoding the cytoskeletal protein filamin A cause diverse malformations in humans. *Nat. Genet.*, **33**, 487–491.
29. Kato, M., Das, S., Petras, K., Kitamura, K., Morohashi, K., Abuelo, D.N., Barr, M., Bonneau, D., Brady, A.F., Carpenter, N.J. *et al*. (2004) Mutations of ARX are associated with striking pleiotropy and consistent genotype–phenotype correlation. *Hum. Mut.*, **23**, 147–159.
30. Neubauer, B.A., Fiedler, B., Himmelein, B., Kampfer, F., Lassker, U., Schwabe, G., Spanier, I., Tams, D., Bretscher, C., Moldenhauer, K. *et al*. (1998) Centrotemporal spikes in families with rolandic epilepsy: linkage to chromosome 15q14. *Neurology*, **51**, 1608–1612.
31. Oleszewski, M., Gutwein, P., von der Lieth, W., Rauch, U. and Altevogt, P. (2000) Characterization of the L1-neurocan-binding site. Implications for L1–L1 homophilic binding. *J. Biol. Chem.*, **275**, 34478–34485.
32. Wei, X.Q., Orchardson, M., Gracie, J.A., Leung, B.P., Gao, Bm., Guan, H., Niedbala, W., Paterson, G.K., McInnes, I.B. and Liew, F.Y. (2001) The Sushi domain of soluble IL-15 receptor alpha is essential for binding IL-15 and inhibiting inflammatory and allogenic responses *in vitro* and *in vivo*. *J. Immunol.*, **167**, 277–282.
33. Hoshino, M., Matsuzaki, F., Nabeshima, Y. and Hama, C. (1993) Hikaru genki, a CNS-specific gene identified by abnormal locomotion in *Drosophila*, encodes a novel type of protein. *Neuron*, **10**, 395–407.
34. Xiong, Z.Q., Qian, W., Suzuki, K. and McNamara, J.O. (2003) Formation of complement membrane attack complex in mammalian cerebral cortex evokes seizures and neurodegeneration. *J. Neurosci.*, **23**, 955–960.
35. Whitney, K.D. and McNamara, J.O. (2000) GluR3 autoantibodies destroy neural cells in a complement-dependent manner modulated by complement regulatory proteins. *J. Neurosci.*, **20**, 7307–7316.
36. Jamali, S., Bartolomei, F., Robaglia-Schlupp, A., Massacrier, A., Peragut, J.C., Regis, J., Dufour, H., Ravid, R., Roll, P., Pereira, S. *et al*. (2006) Large-scale expression study of human mesial temporal lobe

epilepsy: evidence for dysregulation of the neurotransmission and complement systems in the entorhinal cortex. *Brain*, **129**, 625–641.
37. Holden, C. (2004) The origin of speech. *Science*, **303**, 1316–1319.
38. Lai, C.S., Fisher, S.E., Hurst, J.A., Vargha-Khadem, F. and Monaco, A.P. (2001) A forkhead-domain gene is mutated in a severe speech and language disorder. *Nature*, **413**, 519–523.
39. Ferland, R.J., Cherry, T.J., Preware, P.O., Morrisey, E.E. and Walsh, C.A. (2003) Characterization of Foxp2 and Foxp1 mRNA and protein in the developing and mature brain. *J. Comp. Neurol.*, **460**, 266–279.
40. Dellatolas, G., de Agostini, M., Jallon, P., Poncet, M., Rey, M. and Lellonat, J. (1988) Mesure de la préférence manuelle dans la population française adulte. *Revue de Psychologie Appliquée*, **38**, 117–136.
41. Wechsler, D. (1981) *Manual for the Wechsler Adult Intelligence Scale-Revised* (*WAIS-R*). The Psychological Corporation, San Antonio, TX.
42. Wechsler, D. (1974) *The Wechsler Intelligence Scale for Children-Revised* (*WISC-R*), The Psychological Corporation, New York.
43. Wechsler, D. (1989) *Wechsler Preschool and Primary Scale of Intelligence-Revised*, The Psychological Corporation, San Antonio, TX.
44. Goodglass, H. and Kaplan, E. (1983) *The Assessment of Aphasia and Related Disorders*, Lea and Febiger, Philadelphia.
45. Maquet, P., Metz-Lutz, M.N., de Saint-Martin, A., Marescaux, C. and Hirsch, E. (2000) Isotope tracer-techniques in rolandic epilepsy and its variants. *Epileptic Dis.* **2** (Suppl. 1), 55–57.
46. Huppke, P., Kallenberg, K. and Gartner, J. (2005) Perisylvian polymicrogyria in Landau-Kleffner syndrome. *Neurology*, **64**, 1660.
47. Lathrop, G.M. and Lalouel, J.M. (1984) Easy calculations of lod scores and genetic risks on small computers. *Am. J. Hum. Genet.*, **36**, 460–465.
48. Laemmli, U.K. (1970) Cleavage of structural proteins during the assembly of the head of bacteriophage T4. *Nature*, **227**, 680–685.
49. Jay, P., Rougeulle, C., Massacrier, A., Moncla, A., Mattei, M.G., Malzac, P., Roeckel, N., Taviaux, S., Lefranc, J.L., Cau, P. *et al*. (1997) The human necdin gene, NDN, is maternally imprinted and located in the Prader–Willi syndrome chromosomal region. *Nat. Genet.*, **17**, 357–361.